

Stability of Detonation Waves under Chain-Branching Kinetics with Small Initiation Rate

M. M. Lopez Aoyagi, M. M. Alves, M. A. Levy, J. Melguizo-Gavilanes & L. Bauwens
University of Calgary, Canada

1 Motivation

Lengths or times scales characterizing detonation waves originate in the chemical kinetics. However because of temperature sensitivity, the kinetics result in a very wide range of scales. As a result, there is no obvious way to relate experimentally measured relevant scales such as the cell size to the problem data. One scale easily computed is the wave thickness, often defined as the half reaction length. However the half reaction length is typically much shorter than experimental scales. Although significantly more complex, linear stability analysis provides a more complex set of scales, including some transverse ones, while taking into account that the planar wave is normally unstable. In addition, the unstable nature of detonation waves is a crucial feature, which should provide enough motivation for studying stability.

Normal modes stability analysis of detonation waves was introduced by Lee & Stewart [1], for finite rate single step Arrhenius kinetics. Buckmaster & Neves [2] focused upon high activation energy. However typical kinetics are characterized by chain-branching, especially for hydrogen. Stability of chain branched detonations has been analyzed by Short & Quirk [3, 4] for a three step scheme used by Kapila in a study of homogeneous explosions [5]. The scheme [5] shown in detail below includes three steps: initiation, branching and termination. It is relatively simple, enough so that results can be analyzed in detail and related to the effects of the various parameters, yet it captures the essential physics. In most situations, including hydrogen detonations, initiation is quite slow and often stiff. Using an asymptotic formulation based upon initiation being slow has the advantage of facilitating the analysis, but also more importantly, to identify the specific effects of the main chemical process, namely, chain-branching and termination. The slow initiation rate assumption [6] leads to a ZND wave structure in which a relatively thin main reaction zone under chain-branching is preceded by a longer initiation zone and followed by even longer termination. Wavelengths of the order of the main reaction zone thickness are then of smaller magnitude than the distance to the leading shock.

A stability analysis assuming small initiation is performed focusing on modes that resolve the main chain-branching zone. Results exhibit similarities and differences with [3, 4].

2 Reference ZND solution

Density ρ and temperature T are scaled by preshock values (index 0), velocity u by preshock speed of sound c_0 , heat release Q by preshock speed of sound squared, and pressure p by γ times the preshock

pressure, in which γ is the (constant) specific heat ratio. Solving the Rankine-Hugoniot equations using Mach number M as independent variable,

$$\sqrt{T} = \frac{M(\gamma M_0^2 + 1)}{M_0(\gamma M^2 + 1)}, \quad \rho = \frac{M_0^2(\gamma M^2 + 1)}{M^2(\gamma M_0^2 + 1)}, \quad u = \frac{M^2(\gamma M_0^2 + 1)}{M_0(\gamma M^2 + 1)}, \quad p = \frac{\gamma M_0^2 + 1}{\gamma(\gamma M^2 + 1)} \quad (1)$$

With $\gamma p = \rho T$ and $q = (1 - \lambda_1 - \lambda_2)Q$. Scaling the rates by the post-shock termination rate, and length by post-shock velocity divided by post-shock termination rate, the steps are initiation I , branching B and termination T :

$$\frac{u}{u_N} \frac{d\lambda_1}{dx} = -r_I - r_B, \quad \frac{u}{u_N} \frac{d\lambda_2}{dx} = r_I + r_B - r_T \quad (2)$$

$$r_I = \lambda_1 k_I \exp \frac{-E_I}{T}, \quad r_B = \rho \lambda_1 \lambda_2 k_B \exp \frac{-E_B}{T}, \quad r_T = \lambda_2 k_T(p, T) \quad (3)$$

Heat release is associated with termination only. Introducing T_I and T_B , $k_I = \exp E_I/T_I$ and $k_B = \exp E_B/T_B$. At the shock, $\lambda_1 = 1$ and $\lambda_2 = 0$. The heat release parameter Δ is defined as

$$\Delta = \Delta_N - \frac{q}{Q}, \quad \Delta_N = \frac{(M_0^2 - 1)^2}{2M_0^2(\gamma^2 - 1)Q} \quad (4)$$

$$M^2 = \frac{\gamma M_0^2 + 1 \pm \sqrt{2M_0^2(\gamma^2 - 1)Q\Delta}}{\gamma M_0^2 + 1 \mp \gamma \sqrt{2M_0^2(\gamma^2 - 1)Q\Delta}} \quad (5)$$

The lower root describes a deflagration behind a shock. Using ϵ and a , and the variable θ ,

$$\epsilon = \frac{k_I}{k_B} \exp \left(\frac{E_B}{T_N} - \frac{E_I}{T_N} \right), \quad a = \rho_N \exp \left(\frac{E_B}{T_B} - \frac{E_B}{T_N} \right), \quad \theta = \frac{E_B}{T_N} \left(1 - \frac{T_N}{T} \right) \quad (6)$$

initiation is slow in the sense that ϵ is assumed to be much smaller than unity [6], describing either a small multiplier or high initiation activation energy in a unified formulation. Analysis is performed for $a > 1$, i.e. a von Neumann point on the explosion side in the explosion diagram. Using Eqs. (6), chemistry is

$$u \frac{d\lambda_1}{dx} = -\frac{a}{\rho_N} \left(\epsilon \exp \frac{E_I \theta}{E_B} + \rho \lambda_2 \exp \theta \right) \lambda_1 \quad (7)$$

$$u \frac{d\lambda_2}{dx} = \frac{a}{\rho_N} \left(\epsilon \exp \frac{E_I \theta}{E_B} + \rho \lambda_2 \exp \theta \right) \lambda_1 - \lambda_2 k_T \quad (8)$$

$$\frac{1 - M^2}{(\gamma - 1)(1 - \gamma M^2)Q} \frac{dT}{dx} = -\frac{d(\lambda_1 + \lambda_2)}{dx} = k_T \frac{u_N}{u} \lambda_2 \quad (9)$$

For $x = O(1)$ (near the shock),

$$\lambda_2 = \frac{a\epsilon}{\rho_N(a-1)} [\exp(a-1)x - 1], \quad \lambda_1 = 1 - \frac{a\epsilon x}{\rho_N(a-1)} - \frac{\epsilon a^2}{(\rho_N a - 1)^2} [\exp(a-1)x - 1] \quad (10)$$

That solution becomes of order unity when $x \rightarrow O(-\log \epsilon)$. For λ_2 and $1 - \lambda_1$ of order unity, setting $\epsilon = 0$ in Eqs. (7) and (8), and introducing

$$\xi = x + \frac{u_N \log \epsilon}{a - 1} \quad (11)$$

$$u \frac{d\lambda_1}{d\xi} = -a \frac{\rho}{\rho_N} \lambda_1 \lambda_2 \exp \theta, \quad u \frac{d\lambda_2}{d\xi} = a \frac{\rho}{\rho_N} \lambda_1 \lambda_2 \exp \theta - \lambda_2 k_T \quad (12)$$

Eliminating ξ and rearranging, for $a > 1$, [6]

$$\lambda_1 = \exp \int_{\Delta_N}^{\Delta} \frac{\rho}{\rho_N} \frac{a}{k_T} \exp \theta d\Delta \quad (13)$$

From Eq. (13), $\lambda_1 \rightarrow 0$ when $\Delta \rightarrow -\infty$. Since $\Delta = \Delta_N - 1 + \lambda_1 + \lambda_2$ and $\lambda_2 \geq 0$, $\Delta \geq \Delta_N - 1 + \lambda_1$. Since $\Delta = 0$ at a sonic point, the current solution is valid only up to the largest of these two values. In either case, the current approximation is valid only up to a value of λ_1 still positive.

The initiation length is obtained by matching [6]:

$$x = \frac{u_N}{a-1} \log \frac{\rho_N(a-1)^2(\Delta_N - \Delta)}{a\epsilon} - u_N \int_{\Delta_N}^{\Delta} \left[\frac{\rho_N}{\rho} \frac{1}{k_T \lambda_2} - \frac{1}{(a-1)(\Delta_N - \Delta)} \right] d\Delta \quad (14)$$

This solution only exists as long as both Δ and λ_2 are positive. Indeed $\Delta = 0$ corresponds to a sonic point, for a nonzero value of λ_1 . Except for strongly underdriven waves, with sonic point occurring before the end of the chain-branching zone, even before that point is reached, λ_2 becomes negative, with $\Delta = \Delta^*$ still positive. Beyond that point, chain-branching no longer takes place. The termination zone length is of $O(1/\epsilon)$.

Of significance in the stability analysis below, $\xi \rightarrow -\infty$ for $\Delta \rightarrow \Delta_N$, in which case $\lambda_2 \rightarrow (a-1)(\Delta_N - \Delta)$, while $\xi \rightarrow \infty$ for $\Delta \rightarrow \Delta^*$, and $\lambda_2 \rightarrow (1-a^*)(\Delta - \Delta^*)$, where

$$a^* = \frac{a\rho\lambda_1^* \exp \theta^*}{\rho_N} < 1 \quad (15)$$

3 Stability

Stability is analyzed in the usual way [1–3], introducing perturbations and going to Fourier space in time using complex frequency ω , (and in the transverse variable, although results below only consider longitudinal modes). The perturbation equations to the unsteady reactive Euler's equations, together with the rate laws, are written only for the main chain-branching zone, using the space variable ξ , resulting in linear equations

$$\frac{dX}{d\xi} = AX \quad (16)$$

in which column vector X contains density, velocities, pressure and mass fractions perturbations and matrix A has elements $a_{ij} = a_{ij}(x)$ available numerically from the ZND solution. To avoid dealing with an infinite domain, ξ is replaced by Δ as the independent variable. However then, frequencies increase at both ends, when $\Delta \rightarrow \Delta_N$ and Δ^* since in both cases ξ becomes infinite. No matter how small the step size, close to the limit, proper resolution is no longer possible. Near the limit, reaction rates become negligible. Assuming non-reactive acoustics is not appropriate because such an assumption is valid too close to the limit, when the effect of a non-zero growth rate amplifies the perturbation solution to different orders of magnitude. An approximate formulation resolving small values of λ_2 is used.

For $\Delta_N - \Delta = z \ll 1$, at $O(z)$, an approximate solution to the the main chain-branching zone formulation is obtained using the Frobenius method. Because at leading order in z , acoustics play no role in the approximation to the rate equation perturbations, and these only affect mass, momentum and energy through a source term in energy, the roots m correspond to, respectively, the acoustic modes, $m_{\pm} = -i\omega/[(a-1)(u \pm c)]$, the entropy mode $m_1 = -i\omega/(a-1)$ (twice) and a mode associated with the λ_2 perturbation, $m_2 = (a-1-i)\omega/(a-1)$. Because heat release is associated with the latter only,

its amplitude L_2 alone determines forcing in the acoustic problem and the λ_1 perturbation, contributing terms

$$\lambda'_1 = \frac{-aL_2z^{m_2}}{a-1}, \quad u' = -\frac{a-1-i\omega}{(a-1)\rho u}p', \quad p' = \frac{(\gamma-1)(a-1)\rho u^2QL_2z^{m_2}}{u^2(a-1)^2 - c^2(a-1-i\omega)^2} \quad (17)$$

respectively in λ_2 , pressure and velocity perturbations. These provide the necessary boundary conditions, with no additional contribution from the other roots. Since the eigensolutions are only defined up to an arbitrary factor, L_2 is arbitrary, as shown by matching with the near shock solution. When expressed in the near-shock coordinate x , at leading order in z , the perturbations $\lambda'_2 = L_2z^{(a-1-i\omega)/(a-1)}$ and $\lambda'_1 = L_1z^{-i\omega/(a-1)}$ are:

$$\lambda'_2 = L_2\epsilon^{(a-1-i\omega)/(a-1)} \exp\left(\frac{(a-1-i\omega)x}{u_N}\right), \quad \lambda'_1 = L_1\epsilon^{-i\omega/(a-1)} \exp\left(\frac{-i\omega x}{u_N}\right) \quad (18)$$

Thus while the real part only contributes a phase shift, an imaginary part of ω of order unity results in near shock magnitudes that differ from those in the chain-branching region, and these differ between the two perturbations, and also with acoustics.

Writing the complex frequency $\omega = \hat{\omega} + i\sigma$, the growth rate is then $-\sigma$. Assuming perturbations smaller than the steady solution by a factor μ in the main chain-branching zone, these contribute to shock motion at order $\mu\epsilon^{\sigma/(a-1)}$. Indeed, when applying the shock boundary conditions not at $x = 0$ but at $x = O(\mu\epsilon^{\sigma/(a-1)})$ additional terms appear in the mass fraction solutions in Eqs. (10), with magnitudes smaller than acoustics by order ϵ , thus matching the current perturbation, and growing exponentially at the same rate when x becomes large. Because there is no match in magnitudes, solutions for other values of m , including L_1 and resonant acoustics, are set to zero.

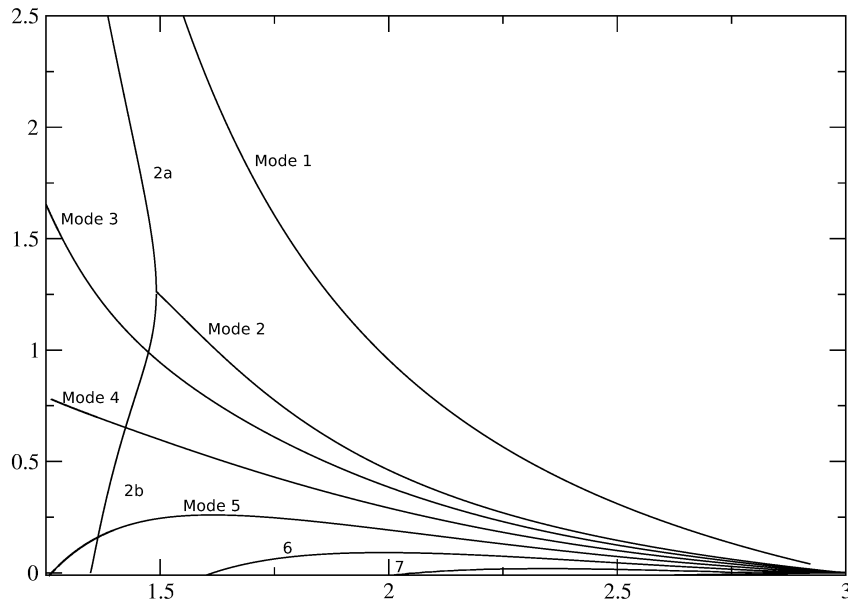


Figure 1: Growth rate vs. T_B . Modes labeled starting with most unstable.

The above is only valid as long as $\sigma = O(1)$. If σ becomes small, then the magnitude of the perturbation becomes uniform so that acoustic reflection at the shock determine the phase shift and the results depend upon ϵ . Likewise, if σ is negative, or if it becomes large, results become invalid.

Boundary conditions for large ξ correspond to no acoustics coming from behind, resulting in an expression accounting for departures from complete reaction [1]. Here it was derived to order $z = \Delta - \Delta^*$, using the Frobenius method. Because two eigenvalues differ by unity and there is a forcing by z times λ'_1 in the equation for λ'_2 , a term in $z \log z$ appears which plays a role in the derivation, but does not appear in the final expression.

Because the reference solution is found numerically as a function of Δ , the perturbation problem also requires numerical solution. Standard fourth order Runge-Kutta method is used. All complex boundary conditions are applied for $\Delta \rightarrow \Delta_N$ except one, for $\Delta \rightarrow \Delta^*$. The two point boundary value eigenvalue problem is solved iteratively using a secant method. The mesh was refined by a factor 16 near the ends, when oscillations in Δ become fast. A step size in Δ of 4×10^{-6} near the ends yields eigenvalues accurate to four significant digits or better. Similar accuracy resulted from switching from the approximate near-boundary formulation to numerical integration over a wide range of values of Δ . An intermediate value was used, 10^{-4} away from the limit.

4 Typical Results

One set of results is shown, for constant termination $k_T = 1$ and $\gamma = 1.2$, $f = 1.0$, $Q = 8$ and $E_B = 12.0$. T_B was varied until reaching the chain-branching limit. (Because the state variables are scaled by preshock values rather than post-shock, the limit T_B differs from unity.) Figure 1 shows growth rate, while Fig. 2, migration diagram.

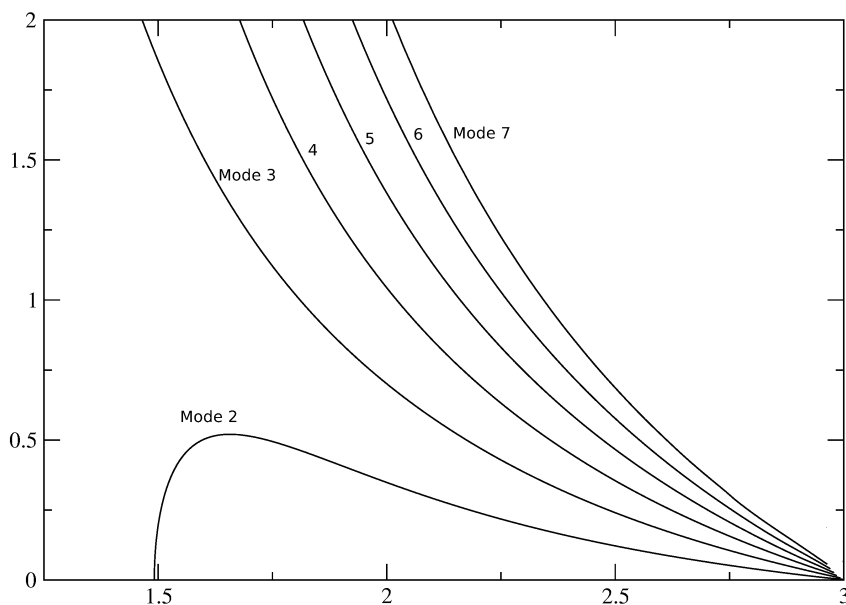


Figure 2: Frequency vs. T_B . Modes labeled as in Fig. 1. Mode 1 has zero frequency (non-oscillatory) hence not shown. Mode 2 also nonoscillatory for $T_B < 1.5$.

Results show presence of a non-oscillatory mode, which is the most unstable. The second most unstable mode turns into two non-oscillatory modes at lower T_B , one of which rapidly becomes stable as T_B is

further decreased. There are an additional five modes. As these become less unstable, their frequency increases. Higher frequency modes are all stable.

5 Conclusion

Stability analysis of ZND detonation waves under a three step chain-branching scheme assuming a small initiation rate shows results typically similar to those of Short et al. [3, 4], with two main differences. First, a non-oscillatory mode remains present even deep within the chain-branching zone. Second, results show clear evidence of a change in behavior when close to the chain-branching limit, with exchange of stability between modes.

A non-oscillatory mode is the most unstable, and there is no sign that the growth rate might eventually stop increasing. However, since time was scaled by the residence time in the main reaction zone, smaller frequencies associated with a longer wavelength such as the initiation zone are not resolved. It is thus possible that the actual frequency of the non-oscillatory modes is of smaller magnitude.

For growth rate of order unity, while the analysis is consistent with reflections at the shock, these do not really affect the results, which are independent of the initiation rate and of the initiation length.

Acknowledgments

Work supported by the Natural Science and Engineering Research Council of Canada and the H2Can Strategic Network.

References

- [1] H. I. Lee & D. S. Stewart, *J. Fluid Mech.* 216 (1990) 103–1232.
- [2] J. D. Buckmaster & J. Neves, *Phys. Fluids* 31 (1988) 3571–3576.
- [3] M. Short & J. J. Quirk, *J. Fluid Mech.* 339 (1997) 89–119.
- [4] M. Short & J. W. Dold, *Math. Comput. Modeling* 24 (1996) 115–123.
- [5] A. K. Kapila, *J. Eng. Mathematics* 12 (1978) 221–235.
- [6] L. Bedard-Tremblay, J. Melguizo-Gavilanes & L. Bauwens, *Proc. Combust. Inst.* 32 (2008) 1669–1676.